Original Research

Combined Dynamic Contrast Enhanced Breast MR and Proton Spectroscopic Imaging: A Feasibility Study

Michael A. Jacobs, PhD,[1]* Peter B. Barker, DPhil,[1,4] Pedram Argani, MD,[2,3] Ronald Ouwerkerk, PhD,[1] Zaver M. Bhujwalla, PhD,[1] and David A. Bluemke, MD, PhD[1]

Purpose: To investigate the feasibility of combined dynamic contrast enhanced (DCE) and magnetic resonance spectroscopy (MRS) in evaluating breast lesions.

Methods: Nine patients with positive mammograms scheduled for either biopsy or mastectomy were examined on a 1.5-T MR scanner. DCE was performed with administration of gadolinium-DTPA contrast using a two-dimensional spoiled gradient recall echo (SPGR) sequence. Proton spectroscopy (TR/TE = 2000/272 msec) was performed using PRESS single slice (10 mm). Lesion time intensity curves were classified as persistent (type 1), plateau (type 2), or washout (type 3) pattern enhancement. Choline (Cho) signal-to-noise ratios (SNRs) and enhancement patterns were compared between benign and malignant lesions as determined by histopathology.

Results: Five patients had breast carcinoma and four had benign lesions. Type 1 enhancement was found in two benign cases, type 2 enhancement in two of four benign and four of five malignant lesions, and one malignant case exhibited a type 3 pattern. Choline SNR was significantly different ($P < 0.003$) between benign and malignant lesions (2.0 ± 0.3 vs. 5.7 ± 1.4; $P < 0.003$). Choline SNR was less than 4.0 in all of the benign lesions, including the two lesions with type 2 enhancement.

Conclusion: Proton MRS appears to be a promising technique for classification of breast lesions when DCE results are equivocal. A combination of DCE and MRS is feasible, and may have improved specificity compared to either modality alone.

Key Words: spectroscopy; magnetic resonance imaging; magnetic resonance spectroscopy; breast blood supply: diagnosis and pathology; neovascularization, pathologic: diagnosis and pathology; computer assisted image processing
J. Magn. Reson. Imaging 2005;21:23–28.
© 2004 Wiley-Liss, Inc.

DYNAMIC CONTRAST-ENHANCED (DCE) magnetic resonance (MR) imaging of the breast has been proposed to increase the specificity of MR imaging for the diagnosis of breast cancer (1–3). Specific patterns of enhancement have been defined as persistent (type 1), plateau (type 2), and washout (type 3) (2,3). Persistent enhancement is characterized by a monotonic increase, plateau enhancement attains a constant level or "plateau," and the washout pattern has a characteristic initial peak followed by an immediate decrease in the signal intensity.

Type 1 contrast enhancement has been shown to be suggestive of a benign lesion, whereas type 3 contrast enhancement is highly associated with breast cancers (2). However, a type 2 plateau enhancement pattern can be seen in both benign and malignant lesions (2). Therefore, in some cases, enhancement patterns may be equivocal and additional diagnostic methods may be needed for clarification.

To overcome these equivocal types of pattern enhancement, morphological characteristics have been employed to differentiate begin from malignant lesions; Nunes et al (4,5), developed an architectural algorithm for differentiating benign vs. malignant breast lesions based upon pattern of enhancement and border characteristics. These were further subdivided into subsets for further classification of architectural characteristics. This model has shown high sensitivity and specificity.

Recent studies using in vivo proton MR spectroscopy (MRS) (6–13) or spectroscopic imaging (MRSI) (14) have demonstrated that Choline (Cho) can be detected in breast cancers, whereas Cho is generally undetectable in normal breast tissue and benign lesions. The detec-

[1]The Russell H. Morgan Department of Radiology and Radiological Science, The Johns Hopkins University School of Medicine, Baltimore, Maryland.
[2]Department of Pathology, The Johns Hopkins University School of Medicine, Baltimore, Maryland.
[3]Department of Oncology, The Johns Hopkins University School of Medicine, Baltimore, Maryland.
[4]F.M. Kirby Research Center for Functional Brain Imaging, Kennedy Krieger Institute, Baltimore, Maryland.
Contract grant sponsor: National Institutes of Health (NIH); Contract grant numbers: 1R01CA100184, P50 CA103175, 1R21CA/RR91798-01.
Presented in part at the 11th Annual Meeting of ISMRM, 10–16 July 2003, Toronto, Canada.
*Address reprint requests to: M.A.J., Ph.D., Department of Radiology, The Johns Hopkins University School of Medicine, Traylor Blg, Rm 217, 712 Rutland Ave, Baltimore, MD 21205. E-mail: mikej@mri.jhu.edu
Received January 15, 2004; Accepted September 28, 2004.
DOI 10.1002/jmri.20239
Published online in Wiley InterScience (www.interscience.wiley.com).

© 2004 Wiley-Liss, Inc.

tion of Cho in breast lesions may therefore aid in differentiation between benign and malignant lesions. Thus, both techniques show promise for distinguishing benign from malignant lesions and the addition of spectroscopy in a breast exam could clarify cases where the contrast enhancement pattern is not definitive.

The purpose of this study was to investigate the feasibility of combining DCE and MRS in analyzing breast lesions.

METHODS AND MATERIALS

Clinical Subjects and Lesion Classification by Histological Analysis

Nine patients (mean and SD; 56 ± 11 years) were referred for MR evaluation of suspicious breast lesions identified by mammography, ultrasound, or clinical breast exam. After the MR study, biopsies were performed on five patients and four patients underwent mastectomy. Lesions were classified as either benign or malignant according to the histologic findings. Benign lesions included fibrocystic changes, benign patterns of duct or lobule distortion, and benign cellular changes (typical or atypical lobular or ductal hyperplasia). Malignant lesions were ductal, lobular, or undifferentiated carcinoma. The protocol was approved by the Institutional Review Board, and informed consent was obtained from all subjects.

MR Imaging

All scans were performed in the prone position on a 1.5-T MR scanner (General Electric Medical Systems; Waukesha, WI), using a dedicated phased array breast coil (Medrad, Pittsburgh, PA). Dynamic MR imaging sequences was performed using a sagittal T1-weighted fast two-dimensional spoiled gradient recall echo (SPGR) sequence (TR/TE/flip angle = 100 msec/4 msec/90°; FOV = 18 × 18 cm, matrix size = 256 × 128; slice thickness = 1.7–2.5 mm; temporal resolution = 15 seconds) obtained before and after intravenous administration of 0.1 mmol/kg gadolinium diethylenetriaminepentaacetic acid (gadopentate dimeglumine [Gd-DTPA]; Berlex Laboratories, NJ). The contrast agent was injected over 10 seconds, with MR imaging beginning immediately after completion of the injection. The contrast bolus was followed by a 20-cc saline flush. Total MR imaging time was 15–30 minutes.

Proton MRS

Single-voxel (SV) spectroscopy (SVS) or MRS imaging (MRSI) was performed on all nine patients. Proton MRSI was performed on a single 10-mm-thick sagittal section using a point resolved spectroscopy sequence (PRESS) for six patients (14). MRSI scan parameters were TR/TE = 2000 msec/272 msec; matrix size = 18 × 18; FOV = 18 cm; and total data acquisition time was approximately 12 minutes. Nominal voxel size was approximately 1.0 cc. The echo signal was digitized with 256 data points and a spectral width of 1000 Hz. Prior to MRSI, shimming was performed to optimize field homogeneity, and water suppression was optimized using automated routines provided by the manufacturer. Water-suppression was accomplished with three sequential chemical shift selective (CHESS) pulses with a bandwidth of 75 Hz, applied on-resonance with the water signal (15). Lipid signals were attenuated by using an inversion pulse (short tau inversion recovery pulse sequence, or STIR) with a delay of 171 msec. Three patients with enhancement patterns allowing the reliable placement of a voxel of 1-mL or more totally within the lesion, were studied using SV PRESS (TR/TE = 2000 msec/272 msec) spectroscopy. The slice and voxel location was defined by a radiologist (D.A.B.) to include the lesion, which usually was most visible on the contrast-enhanced scans (i.e., all spectroscopy studies were performed after contrast administration).

MR and Spectroscopic Data Analysis

MR image analysis was performed using a SUN UltraSPARC60 workstation (Sun Microsystems, Mountain View, CA) and processed using the Eigentool image analysis software (Image Analysis Lab, Henry Ford Hospital, Detroit MI) (16,17). Subimaging of the breast from the background was done using thresholding and morphological operations (18). After subimaging, an inhomogeneity correction method was applied to the MR imaging data set (19). Lesion size was determined from the postcontrast MR images. Regions of interest (ROIs) were defined for the adipose and lesion tissue and were used to generate mean signal intensity values for dynamic contrast enhanced images. Lesion ROIs were determined from the areas of greatest lesion enhancement by a board certified body radiologist (D.A.B.) blinded to the spectroscopy results. Enhancement of the lesion was classified as malignant if there was a focal mass with irregular or spiculated margins, if enhancement was in a ductal distribution, if a solid lesion showed rim enhancement, or if there was intense regional enhancement in less than one quadrant. Enhancement of the lesion was classified as benign if a focal mass showed smooth or lobulated margins with internal septations, or if the mass was cystic. Breast lesions not fitting criteria of either malignant or benign were considered indeterminate. For dynamic MR images, lesions that showed a washout or plateau curve were classified as malignant. Lesions with delayed or indeterminate enhancement were classified as benign (2,3).

The spectroscopic data were reconstructed using in-house software (P.B.B.) on a Sun ULTRA SPARC 60 computer system (Sun Microsystems, Mountain View, CA). The spectroscopy data sets were processed by three-dimensional Fourier transformation, with cosine filters in the spatial (phase-encoding) domains after zero-filling to a 32 × 32 matrix size, and exponential line broadening of 3 Hz, zero-filling to 2048 data points, and a high-pass convolution filter to remove the residual water signal (50 Hz stop-band) in the time-domain. After setting the chemical shift of water to 4.7 ppm, spectroscopic images (Figs. 1 and 2) were created by numerical integration over the following frequency ranges: choline (Cho, 3.14–3.34 ppm); lipids (0.0–1.45 ppm); and water (4.2–5.2 ppm). For display, metabolic images were linearly interpolated to 256 × 256 points.

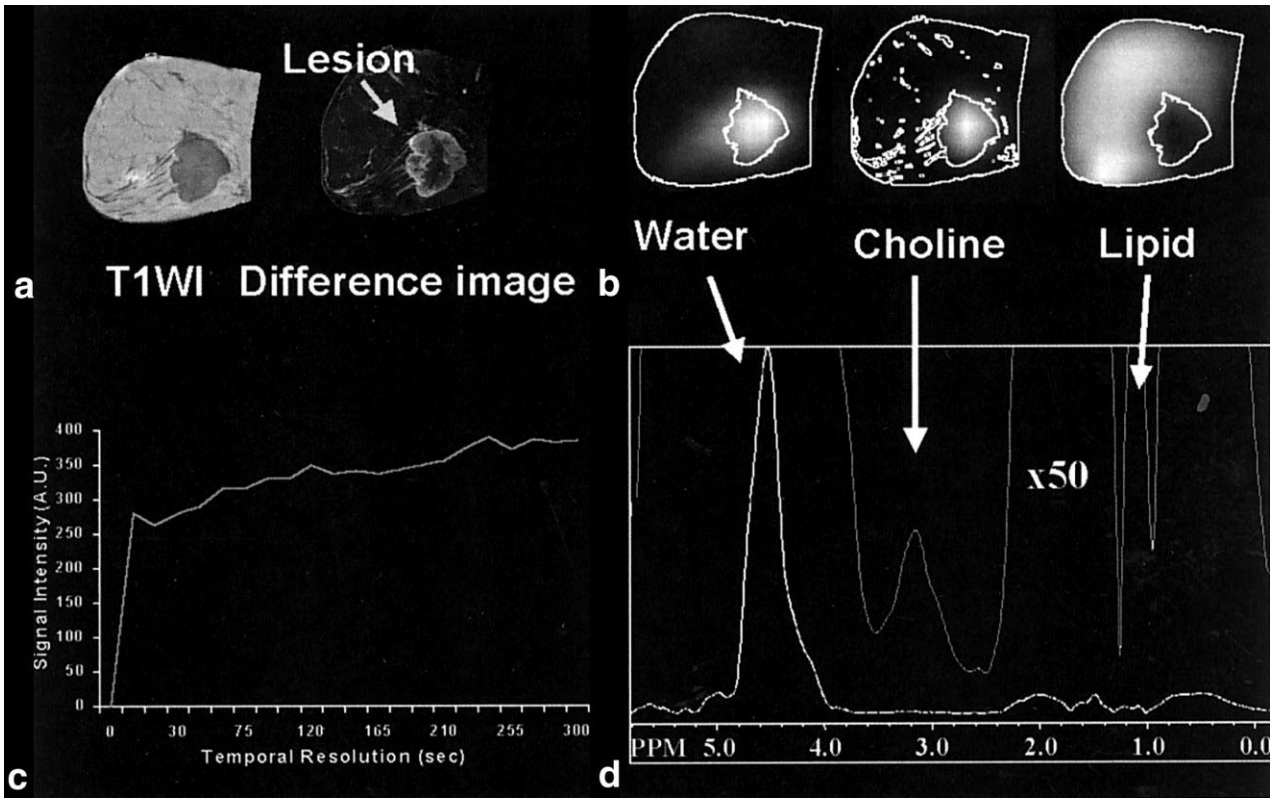

Figure 1. Dynamic contrast MR and proton MRSI in a 62-year-old patient (patient #8) with invasive ductal carcinoma. **a:** T1-weighted pre-Gd-DTPA dynamic contrast (DCE) MR image and the subtracted DCE MR image for lesion localization. **b:** MRSI images of water, choline, and lipids. **c:** Pattern enhancement curve from the lesion and fatty tissue. Signal intensity values were obtained from the area of greatest enhancement. This patient had a type 1 (persistent) enhancement pattern. **d:** Representative spectrum and magnified (50×) region demonstrates a detectable Cho signal (SNR = 7.5) in the lesion at 3.2 ppm.

The criteria for determining the presence or absence of Cho were that a peak height should be clearly identifiable above baseline noise at 3.2 ppm within the lesion. The peak height of the signal in the Cho frequency range in one voxel localized completely within the lesion was quantified using a simplex curve-fitting routine and expressed as a ratio relative to the background noise level between 7.0 and 9.0 ppm (where no signals are expected) in the same voxel.

Statistical Analysis

Descriptive statistics consisted of means and SDs for patient demographics. A two-tailed, unequal variance *t*-test was employed to determine whether Cho SNR was different for malignant versus benign lesions. Statistical significance was set at $P < 0.05$.

RESULTS

Five patients were diagnosed with invasive breast carcinoma (tumor grade range = 1–3) and four patients with benign lesions (Table 1). The average lesion size was 3.1 ± 1.7 cm. Two benign lesions exhibited type 1 (persistent) enhancement. Two of four benign and four of five malignant lesions had a type 2 (plateau). One malignant case exhibited a type 3 (washout) pattern. Three malignant lesions had irregular shapes and the other malignant lesions had lobular or round shapes, respectively. Two of the benign lesions had lobulated shapes and the other two had round shapes.

Figure 1 shows a representative patient with invasive ductal carcinoma (tumor grade = 3) that exhibited a persistent (type 2) enhancement. The lesion had a lobular shape. MRSI metabolic image demonstrated the presence of choline within the breast lesion. A second example is shown in Fig. 2 from a patient with invasive ductal carcinoma (tumor grade = 3). The lesion exhibited a plateau pattern of enhancement (type 2), but had an irregular shape. Cho signal was detectable in the lesion. There was a significant difference between the Cho SNR of benign and malignant lesions($P < 0.003$). However, there was no significant differences between the lesion size of the two groups ($P = 0.3$).

Figure 3 shows a breast lesion with rim enhancement and persistent (type 1) enhancement pattern. Spectroscopy did not detect Cho in the lesion and the histological analysis of the tissue was benign breast tissue with fibrocystic changes.

Choline was detected in four of the five confirmed cases of breast cancer. All of the benign cases (four of four) failed to show a detectable choline signal. In the two cases of type 1 enhancement pattern, Cho was not detected. In addition, in breast lesions presenting with a type 2 enhancement pattern, choline was detected by spectroscopy in three of four malignant lesions but not in any of the benign cases (two of two).

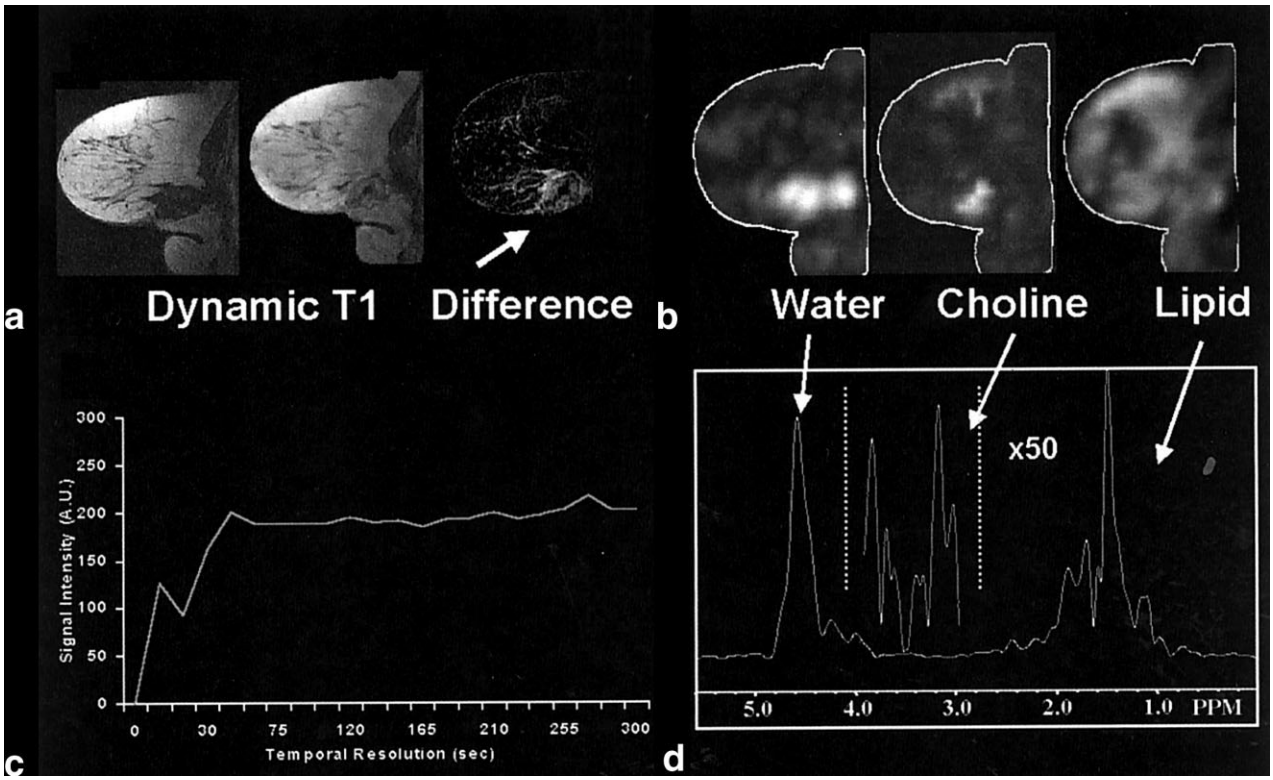

Figure 2. Dynamic contrast MR and proton MRSI in a 63-year-old patient with invasive ductal carcinoma (patient #7) **a:** T1-weighted Gd-DTPA dynamic contrast (DCE) MR image and the subtracted DCE MR image for lesion localization. **b:** MRSI images of water, choline, and lipids. **c:** Pattern enhancement curve from the lesion and fatty tissue. Signal intensity values were obtained from the area of greatest enhancement. This patient had a type 2 (plateau) enhancement pattern. **d:** Representative spectrum and magnified (50×) region demonstrates a detectable Cho signal (SNR = 6.6) in the lesion at 3.2 ppm.

DISCUSSION

The current pilot study suggests that spectroscopy can be combined with DCE MR to provide additional information in the diagnosis in breast cancer. Choline is known to be elevated in many types of neoplasms (20–24). Proton single voxel (6–10,13,25–27) and multivoxel spectroscopy (14) has been shown to be a sensitive and specific technique for the diagnosis of breast cancer based upon the detection of a Cho signal.

However, none of these previous studies combined spectroscopy with DCE curve analysis. The current study indicates that a multiparametric approach using MRS and DCE MR can provide important information about the metabolic status of breast tissue that may increase the specificity of MR for breast cancer diagnosis. However, larger studies are needed to verify the initial finding of this report, as shown in a recent study using SVS (28).

Although our patient population was small, some interesting results emerged. For instance, one patient exhibited peripheral rim enhancement with type 1 pattern. Rim enhancement is highly suggestive of malig-

Table 1
Patient Demographics and MR Characteristics, and Histological Results

Patient	Age	Tumor size (cm)	Shape	CE type	Choline SNR	Tumor grade	Histology
1	48	1.8	Lobulated	1	1.8	—	Fibroadenoma
2	61	2.9	Lobulated	2	2.4	—	Benign with fibroadenomatoid change
3	53	1.0	Round	2	1.7	—	Fibrocystic change
4	63	4.0	Round	2	2.0	—	Benign with focal fibrosis
5	34	5.0	Irregular	3	4.5	3	Invasive ductal carcinoma
6	72	2.0	Irregular	2	4.1	1	Invasive ductal carcinoma
7	63	3.8	Irregular	2	6.6	3	Invasive ductal carcinoma
8	62	6.0	Lobulated	1	7.5	3	Invasive ductal carcinoma
9	52	1.3	Round	2	5.9	1	Invasive ductal carcinoma
Mean	56	3.1					
SD	11	1.7					

CE = contrast enhancement types, shape = tumor size, morphological characteristics, Cho SNR = choline peak signal-to-noise ratio.

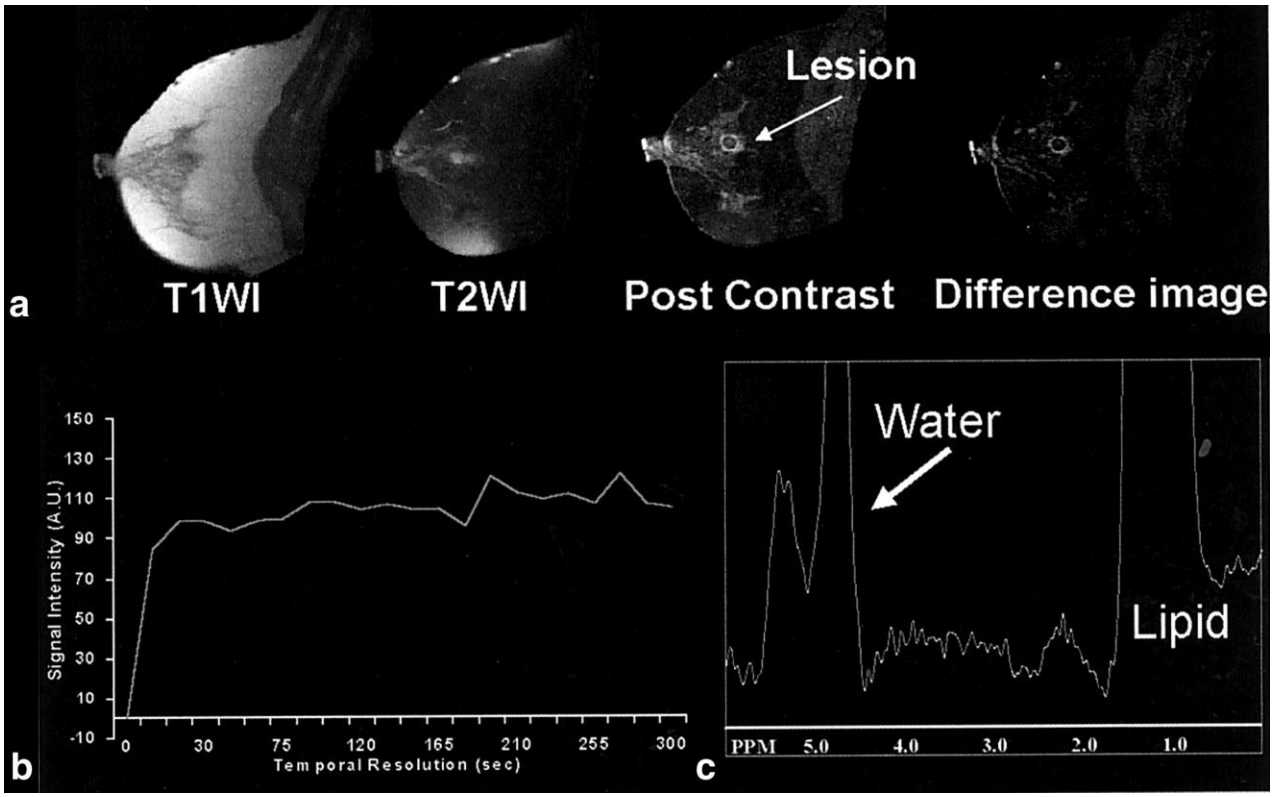

Figure 3. a: Dynamic contrast MR demonstrates a breast lesion with rim enhancement. **b:** Plateau (type 2) enhancement pattern in a 53-year-old patient (patient #3). Signal intensity values were obtained from the area of greatest enhancement. **c:** Spectroscopy detected no Cho signal (SNR = 1.7) at 3.2 ppm in representative spectrum and magnified (50×) region in the lesion. Histological analysis of the tissue was benign breast tissue.

nancy (4,29). However, no Cho was detected in the lesion and was diagnosed benign by histological analysis. Also, spectroscopy was able to detect Cho in breast lesions with a type 2–enhancement pattern that on histology were subsequently diagnosed as cancer. It has been suggested that dynamic breast imaging is not a "standalone" method for diagnosing breast cancer and should be used with other imaging techniques (2,3), especially morphologic characteristics. In this study, we observed that two of the malignant lesions had shapes indicative of benign lesions. Thus, the metabolic information provided by MRSI added specificity to these lesions that were otherwise misclassified.

The current study used a combination of MRSI and SVS for breast lesion evaluation. Potential advantages of MRSI over SVS include the ability to evaluate multiple lesions simultaneously and the ability to gauge the extent of disease infiltration into surrounding tissue. However, significant technical problems exist for MRSI of the breast, particularly relating to water and lipid suppression (30), field homogeneity, whole breast coverage in acceptable scan times, and quantitation. The wings or sidebands of the much larger residual water and lipid signals could lead to ambiguous detection of the Cho signal because of the overlap. We attempted to minimize this by using a long echo time (TE = 272 msec) and STIR to null lipids lipid sidebands, however, improved methods of water and lipid suppression for breast MRSI will help in the definitive identification of Cho, such as TE averaging (30) or spectral saturation methods (31).

Finally, we recognize that a potential limitation of the current study is that spectroscopy was performed after contrast administration (since spectroscopy locations were centered on lesions that were best visualized on contrast-enhanced MRI). Although there have been no systematic studies of the effect of Gd-DTPA on the spectra of breast lesions, we expect the effect to be small, since either no or very small changes in Cho in enhancing brain tumors were noted after Gd-DTPA administration (32,33). In addition, successful post-Gd-DTPA single-voxel MRS of breast lesions has been previously reported (6). Metabolites (choline) are expected to be located in the intracellular space, while Gd-DTPA is in the extracellular space, so it is expected that the effect of Gd-DTPA on the MRSI signal is limited to remote, T_2* effects (34) rather than T_1 effects, which would require direct interaction of Cho and Gd-DTPA molecules. In conclusion, proton spectroscopy of the breast may be useful as an adjunct diagnostic procedure in dynamic breast imaging in equivocal cases for the differential diagnosis of enhancing lesions to increase the specificity of breast MR and be easily incorporated into a multiparametric approach for breast cancer identification and classification (35).

ACKNOWLEDGMENTS

We thank Cindy Maranto and Cheryl Arnold for their assistance in obtaining the MR data. We thank Lucie Bower, Dr. Donald Peck, and Dr. Hamid Soltanian-Zadeh, Henry Ford Hospital, Detroit, Michigan, for the

Eigentool image analysis software used for image processing. This work was supported in part by NIH 1R01CA100184 (to M.A.J.), P50 CA103175 (career development award to M.A.J./Z.A.B.) and 1R21CA/RR91798-01 (to P.B.B.).

REFERENCES

1. Boetes C, Barentsz JO, Mus RD, et al. MR characterization of suspicious breast lesions with a gadolinium-enhanced TurboFLASH subtraction technique. Radiology 1994;193:777–781.
2. Kuhl CK, Mielcareck P, Klaschik S, et al. Dynamic breast MR imaging: are signal intensity time course data useful for differential diagnosis of enhancing lesions? Radiology 1999;211:101–110.
3. Orel SG. Differentiating benign from malignant enhancing lesions identified at MR imaging of the breast: are time-signal intensity curves an accurate predictor? Radiology 1999;211:5–7.
4. Nunes LW, Schnall MD, Orel SG, et al. Breast MB imaging: interpretation model. Radiology 1997;202:833–841.
5. Nunes LW, Schnall MD, Orel SG. Update of breast MR imaging architectural interpretation model. Radiology 2001;219:484–494.
6. Yeung DK, Cheung HS, Tse GM. Human breast lesions: characterization with contrast-enhanced in vivo proton MR spectroscopy—initial results. Radiology 2001;220:40–46.
7. Thomas MA, Binesh N, Yue K, DeBruhl N. Volume-localized two-dimensional correlated magnetic resonance spectroscopy of human breast cancer. J Magn Reson Imaging 2001;14:181–186.
8. Cecil KM, Schnall MD, Siegelman ES, Lenkinski RE. The evaluation of human breast lesions with magnetic resonance imaging and proton magnetic resonance spectroscopy. Breast Cancer Res Treat 2001;68:45–54.
9. Gribbestad IS, Sitter B, Lundgren S, Krane J, Axelson D. Metabolite composition in breast tumors examined by proton nuclear magnetic resonance spectroscopy. Anticancer Res 1999;19:1737–1746.
10. Roebuck JR, Cecil KM, Schnall MD, Lenkinski RE. Human breast lesions: characterization with proton MR spectroscopy. Radiology 1998;209:269–275.
11. Kvistad KA, Bakken IJ, Gribbestad IS, et al. Characterization of neoplastic and normal human breast tissues with in vivo (1)H MR spectroscopy. J Magn Reson Imaging 1999;10:159–164.
12. Katz-Brull R, Lavin PT, Lenkinski RE. Clinical utility of proton magnetic resonance spectroscopy in characterizing breast lesions. J Natl Cancer Inst 2002;94:1197–1203.
13. Kim JK, Park SH, Lee HM, et al. In vivo 1H-MRS evaluation of malignant and benign breast diseases. Breast 2003;12:179–182.
14. Jacobs MA, Barker PB, Bottomley PA, Bhujwalla Z, Bluemke DB. Proton MR spectroscopic imaging of human breast cancer: a preliminary study. J Magn Reson Imaging 2004;19:68–75.
15. Haase A, Frahm J, Hanicke W, Matthaei D. H-1-Nmr chemical-shift selective (CHESS) imaging. Phys Med Biol 1985;30:341–344.
16. Jacobs MA, Knight RA, Windham JP, et al. Identification of cerebral ischemic lesions in rat using eigenimage filtered magnetic resonance imaging. Brain Res 1999;837:83–94.
17. Windham JP, Abd-Allah MA, Reimann DA, Froelich JW, Haggar AM. Eigenimage filtering in MR imaging. J Comput Assist Tomogr 1988;12:1–9.
18. Jacobs MA, Knight RA, Soltanian-Zadeth H, et al. Unsupervised segmentation of multiparameter MRI in experimental cerebral ischemia with comparison to T2, Diffusion, and ADC MRI parameters and histopathological validation. J Magn Reson Imaging 2000;11:425–437.
19. Jacobs MA, Windham J, Soltanian-Zadeth H, Peck D, Knight R. Registration and warping of magnetic resonance images to histological sections. Med Phys 1999;26:1568–1578.
20. Gill SS, Thomas DG, Van Bruggen N, et al. Proton MR spectroscopy of intracranial tumours: in vivo and in vitro studies. J Comput Assist Tomogr 1990;14:497–504.
21. Kurhanewicz J, Vigneron DB, Nelson SJ, et al. Citrate as an in vivo marker to discriminate prostate cancer from benign prostatic hyperplasia and normal prostate peripheral zone: detection via localized proton spectroscopy. Urology 1995;45:459–466.
22. Mukherji SK, Schiro S, Castillo M, Kwock L, Muller KE, Blackstock W. Proton MR spectroscopy of squamous cell carcinoma of the extracranial head and neck: in vitro and in vivo studies. AJNR Am J Neuroradiol 1997;18:1057–1072.
23. van Zijl PC, Moonen CT, Gillen J, et al. Proton magnetic resonance spectroscopy of small regions (1 mL) localized inside superficial human tumors. A clinical feasibility study. NMR Biomed 1990;3:227–232.
24. Aboagye EO, Bhujwalla ZM. Malignant transformation alters membrane choline phospholipid metabolism of human mammary epithelial cells. Cancer Res 1999;59:80–84.
25. Kvistad KA, Bakken IJ, Gribbestad IS, et al. Characterization of neoplastic and normal human breast tissues with in vivo H-1 MR spectroscopy. J Magn Reson Imaging 1999;10:159–164.
26. Jagannathan NR, Kumar M, Raghunathan P, Coshic O, Julka PK, Rath GK. Assessment of the therapeutic response of human breast carcinoma using in vivo volume localized proton magnetic resonance spectroscopy. Curr Sci 1999;76:777–782.
27. Gribbestad IS, Singstad TE, Nilsen G, et al. In vivo 1H MRS of normal breast and breast tumors using a dedicated double breast coil. J Magn Reson Imaging 1998;8:1191–1197.
28. Huang W, Fisher PR, Dulaimy K, Tudorica LA, O'Hea B, Button TM. Detection of breast malignancy: diagnostic MR protocol for improved specificity. Radiology 2004;232:585–591.
29. Orel SG, Schnall MD, LiVolsi VA, Troupin RH. Suspicious breast lesions: MR imaging with radiologic-pathologic correlation. Radiology 1994;190:485–493.
30. Bolan PJ, DelaBarre L, Baker EH, et al. Eliminating spurious lipid sidebands in 1H MRS of breast lesions. Magn Reson Med 2002;48:215–222.
31. Barker PB, Smith M, Gillen J, Jacobs MA. A protocol for quantitative 3D MR spectroscopic imaging of the human breast. In: Proceedings of the 45th Experimental Nuclear Magnetic Conference. ENC, 2004. p 221.
32. Smith JK, Kwock L, Castillo M. Effects of contrast material on single-volume proton MR spectroscopy. AJNR Am J Neuroradiol 2000;21:1084–1089.
33. Sijens PE, Oudkerk M, van Dijk P, Levendag PC, Vecht CJ. 1H MR spectroscopy monitoring of changes in choline peak area and line shape after Gd-contrast administration. Magn Reson Imaging 1998;16:1273–1280.
34. Akbudak E, Norberg RE, Conturo TE. Contrast-agent phase effects: an experimental system for analysis of susceptibility, concentration, and bolus input function kinetics. Magn Reson Med 1997;38:990–1002.
35. Jacobs MA, Barker PB, Bluemke DA, Maranto C, Arnold C, Herskovits EH, Bhujwalla Z. Benign and malignant breast lesions: diagnosis with multiparametric MR imaging. Radiology 2003;229:225–232.